Breakthrough Report

Title: Protein reservoirs of seeds are composites of amyloid and amyloid-like structures facilitating germination

Author names and affiliations: Nabodita Sinha[a], Talat Zahra[a], Avinash Yashwant Gahane[a], Ashwani Kumar Thakur[a*]

[a]Department of Biological Sciences and Bioengineering, Indian Institute of Technology Kanpur, UP-208016, India.

***Corresponding author:** Prof. A.K.Thakur (akthakur@iitk.ac.in)

Running title: Amyloidic composites facilitate germination in seeds

Abstract

The functional roles of amyloids are known across diverse species, but their natural presence in plants remains underexplored. Based on the structure and function of protein bodies found in other organisms, we hypothesize that the seed storage protein bodies (SSPB) may have amyloid structures for controlling physiological functions. Here we show that monocot and dicot SSPB exhibit a speckled-pattern of amyloids interspersed in an amyloid-like matrix, suggesting their composite nature. This is confirmed by amyloid-specific probes, amyloidogenic region scans, infrared signatures, reconstitution studies, and differential degradation during germination. The role of amyloidic composites in seed germination is proved by amyloid content, degradation inhibition and relevant germination parameters, using *in-vitro* SSPB, *ex-vivo* protoplasts and *in-situ* seed sections. The results open new research questions in understanding molecular details of SSPB assembly-disassembly and utilization, in addition to evolutionary roles of amyloid structure and function.

Introduction:

The original study of seed storage proteins in monocots and dicots can be traced back to the 18th century.(1, 2) The seed storage protein bodies (SSPB) of aleurone cells in monocots are comprised of storage proteins including globulins,(3) minerals and lipids.(4, 5) In dicot seeds, the cotyledon cells contain a protein matrix,(6) composed of SSPB of mostly globulins.(7, 8) Most of these proteins are targeted to the SSPB in association with the Golgi apparatus, leading to the formation of aggregated electron-rich structures.(1, 9) Similar structures of electron-rich aggregates of proteins are found in diverse species, ranging from bacteria to humans.(10) Interestingly, some of them also act as storage reservoirs. For example, metabolic enzymes assemble into aggregates to protect the proteins,(11) while proteasome storage granules sequester and store the proteasomes for safe-keeping.(12) These aggregates or inclusions are categorized as amyloids or amyloid-like structures to perform functions of storage and stability. Whereas amyloids are proteinaceous cross-β sheet rich aggregates and exhibit apple green birefringence with Congo red, amyloid-like aggregates might lack one or more of the key characteristics of amyloids.(13, 14) Although, there are reports suggesting specific protein-protein interactions to

form SSPB, (4) it is not yet clear whether they have amyloid, amyloid-like or amorphous structures. Because the protein bodies of bacteria, yeast, and even humans are often associated with amyloid or amyloid-like aggregates, we hypothesize that the plant SSPB might also possess amyloids for performing functional roles.

To detect amyloids in plants, previous reports used experimental conditions to induce protein aggregation *in-vitro* or used single probe for *in-vivo* analysis.(15) These limited findings and experimentations do not reflect the inherent amyloidic nature of the plant proteins *in-vivo*.(16) Moreover, functional aspects of endogenous amyloids in plant are also lacking. Since hormones and proteases play a major role in the maintenance/degradation of SSPB and subsequent germination, the effect of these molecular players on the amyloidic aggregates need to be understood.(17) For this purpose, seed protoplasts are an ideal choice since these are free of cell wall and the presence of these structures in the seed tissues, might lead to amyloid staining misperceptions. Also, protoplasts represent a dynamic active metabolic state and can be utilized to capture the effect of the exogenous effector molecules. In this study, we have used a combinatorial approach of multiple amyloid-specific probes and shown that the seed sections and protoplasts of wheat (*Triticum aestivum,* monocot), barley (*Hordeum vulgare,* monocot) chickpea (*Cicer arietinum,* dicot) and mungbean (*Vigna radiate,* dicot) exhibit intense amyloidic signatures in the SSPB of the aleurone and cotyledon cells. The amyloid-specific spectroscopic characteristics in the isolated SSPB, further bolsters the hypothesis. Moreover, the differential degradation of amyloid-like and amyloids during seed germination and elucidation of an amyloid-degradation dependent germination percentage confirms the critical role of amyloids in seed germination.

Results:

Detection and confirmation of amyloid presence in seed sections using combinatorial amyloid-specific probes: Before using amyloid-specific probes to detect amyloid presence in SSPB, the seed tissue sections were dual stained with acid fuchsin and calcofluor white to visualize the proteinaceous and cellulose-rich regions.(18) It is important to demarcate these two biochemical compartments, since cellulose also binds to Congo red (CR), a gold-standard dye for

amyloids.(18) As shown in **Figure 1**, the seed coat, aleurone layer, and endosperm cytoplasm of monocot **(Figure 1 a1-a3)** and cotyledon cell-matrix of dicot seed sections **(Figure 1 b1-b3)** are stained with acid fuchsin and exhibit a pinkish-magenta colour on binding with proteins. Calcofluor white staining leads to a blue-fluorescence in the cell wall regions of monocots **(Figure 1 a3)** and dicots **(Figure 1 b3)** and represent cellulose-rich regions**.** To further confirm the integrity and structural aspects of the seed sections, scanning electron microscopy (SEM) was performed on wheat and mungbean. In **Figure 1 c1 and c2,** protein matrix of the aleurone and cotyledon cells is visibly intact, and corroborates with the SSPB structures observed in the literature.(19)

To demarcate amyloid or amyloid-like deposits in the seeds, we chose Thioflavin-T (ThT) as the first probe. It is one of the most popular dyes for amyloid or amyloid-like deposit detection and studying *in-vitro* aggregation kinetics.(20) ThT dataset was validated by another molecular rotor, Proteostat®. It is a recently discovered probe, designed to detect intracellular and extracellular amyloids or amyloid-like deposits even if the amyloidogenic proteins are sparse.(21, 22) For detecting amyloids or amyloid-like aggregates in seeds, wheat **(Figure 1 d1-d2),** barley **(Figure 1 d3-d4),** chickpea **(Figure e1-e2)** and mungbean **(Figure e3-e4)** seed sections were stained with ThT and visualized using a confocal microscope. In case of the monocot seeds, intense fluorescence intensity was observed in the aleurone layer. The subaleurone layer shows intermediate fluorescence while the endosperm tissue shows minimum ThT signal. The fluorescence intensity was further quantified for each of these tissues to confirm this. **(Figure 1 f1-f2)** In the dicot seed sections, the cotyledon cell matrix produces an intense green fluorescence. In Proteostat® stained sections, the images show comparable pattern similar to ThT stained seed sections of barley **(Figure 1 g1)**, and chickpea **(Figure 1 g2)**, confirming the presence of amyloid or amyloid-like structures in SSPB. As positive control, human abdominal fat biopsy of a positive amyloid patient, **(Figure 1 h1-h2)** (23) and amyloidic fibrils of Sup35-N terminal fragment GNNQQNY **(Figure 1 h3-h4)** were stained with ThT and Proteostat® probes with same parameters as seed samples**.** Potato tubers **(Figure 1 h5-h6)** are chosen as the negative control, since these are rich in carbohydrates instead of proteins.(24) Monocot endosperm tissue was used as another negative control, since it shows minimum signal with both probes **(Figure 1 h7-h8)**. ThT and Proteostat® staining therefore suggests that both monocot and dicot seeds contain inherent amyloidic structures.

The diagnostic relationship between amyloids and Congo red (CR) is historical and goes back to 1922 when this dye was used to stain amyloids and exhibited salmon-pink or red color in bright-field microscopy.(25) Subsequently, the optical anisotropy of amyloids on binding with CR and the resulting signature of apple-green birefringence enabled it as one of the most reliable methods for detection of amyloids in tissues and clinical samples.(13, 26) To confirm the presence of amyloids in the SSPB of aleurone and the cotyledon cells, seed sections were stained with CR and the samples were visualized between two polarizers.(13, 26) A characteristic apple-green birefringence of amyloids was observed in the aleurone SSPB of wheat **(Figure 1 a-d)** and barley **(Figure 1 e-h) (Supplemental Movie 1 and 2).** Fascinatingly, unlike ThT and Proteostat® staining, which showed intense signal in the whole proteinaceous region of the aleurone cells, CR-induced birefringence was observed in some of these regions. Similar case was observed for the cotyledon cells of chickpea **(Figure 1 i-l)** and mungbean **(Figure 1 m-p) (Supplemental Movie 3 and 4)**. The presence of CR-stained amyloids interspersed between amyloid-like structures suggests a composite structure in seed storage proteins. As positive control, the same human fat biopsy tissue **(Figure 1 q1-q2)** and Sup35 N-terminal domain heptapeptide fibrils are represented **(Figure 1 q3-q4)** which exhibit the characteristic apple-green birefringence of amyloids. For negative control, potato tuber **(Figure 1 q5-q6)** and wheat endosperm sections were utilized where negligible birefringence is observed **(Figure 1 q7-q8).**

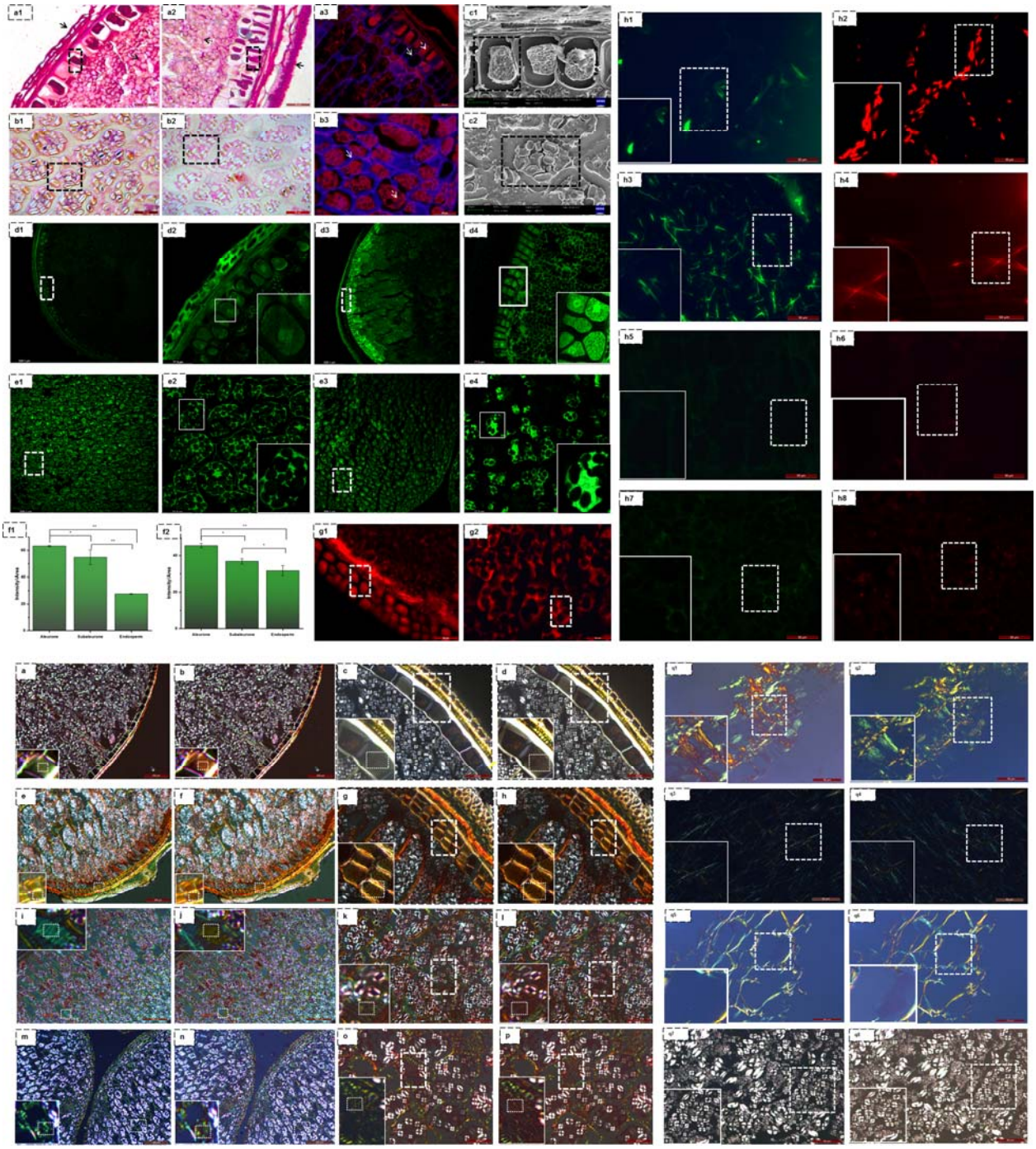

Figure 1 Analysis of amyloid structures in proteinaceous regions of seed sections. The protein-specific dye, acid fuchsin, exhibits characteristic magenta color in the seed coat (solid black arrow), aleurone (black dashed boxes), and sub-aleurone layer (black dashed arrow) of wheat (*Triticum aestivum*) (a1) and barley (*Hordeum vulgare*) (a2). In the dicot seeds, the stain is visible in the SSPB of cotyledon cells (black dashed boxes) of chickpea (*Cicer arietinum*) (b1) and mungbean (*Vigna radiata*) (b2). Acid fuchsin stains the aleurone and cotyledon cells prominently, exhibiting the proteinaceous deposits in these cells. In dual staining of acid fuchsin and calcofluor white, the barley aleurone cells (a3) and mungbean cotyledon cells (b3) exhibit red fluorescence in proteinaceous regions, whereas calcofluor white produces blue fluorescence in cell wall regions. Solid white arrows represent cell walls, whereas

dashed white arrows represent the SSPB. SEM (Scanning Electron Microscopy) analysis of wheat (c1) and mungbean (c2) reveal that the structure of the aleurone and cotyledon cells is maintained after histological processing. Gamma value for each bright-field image ranges from 0.6-0.9, the changes in brightness/contrast has been applied to the whole image. **ThT** staining of monocot seeds reveals that both wheat (d1-d2 and f1) and barley (d3, d4 and f2) exhibit an intense fluorescence in the aleurone layer compared to the endosperm cells, suggesting an enrichment of amyloid-like protein aggregates in the aleurone layer. The dicot seeds of chickpea (e1 and e2) and mungbean (e3 and e4) exhibit an intense signal in the SSPB of cotyledons. The white dashed boxes represent intense fluorescing areas of 10X magnified images and white solid lined boxes represent similar areas in 40X magnified images. The insets represent magnified portions of the solid-lined boxes. The bar graphs represent each type of tissue's intensity/area ratio, i.e., for aleurone, subaleurone and endosperm. The ratio of five z-stacks are averaged for this purpose and plotted as bar graphs with error bars representing standard error of the mean. Student's t-test is performed for statistical analysis. In (f1) *p=0.02, **p=0.003; (f2) *p=0.01, **p=0.003) Gamma and intensity value for each confocal image is kept same for quantification purposes. **Proteostat®** staining exhibits that the monocot seeds of barley (g1) and dicot seeds of chickpea (g2) demonstrate the presence of possible amyloids or amyloid-like aggregates in the SSPB of aleurone and cotyledon cells as evident from the red fluorescence in these areas. White dashed boxes represent the intense signal in a representative area. As positive controls of Tht and Proteostat®, human abdominal fat biopsy tissue of a positive amyloidosis patient (h1, h2) and amyloidic fibrils of Sup35-N-terminal domain peptide (GNNQQNY) is represented (h3, h4), showing intense green or red fluorescence due to positive staining. As negative controls of the two probes, sections of potato tuber as a storage organ (h5, h6) and the wheat endosperm is represented (h7, h8) where, negligible fluorescence is observed. Gamma values for each ThT and Proteostat® image ranges from 1.8-2.5 to bring uniformity, changes in brightness/contrast has been applied to the whole image. **Confirmation of amyloids in seed sections by CR staining**. Left two panels represent the apple-green to red birefringence when the sample is placed between two polarisers at 10X magnification. The right two panels show the same at 40X magnification. Both wheat (*Triticum aestivum*) (a-d) and barley (*Hordeum vulgare*) (e-h) aleurone cells show a visible change in the apple-green birefringence, characteristic of amyloids as indicated by the white dashed boxes inside the insets. Similar changes in birefringence are observed in some regions of the SSPB of cotyledon cells of chickpea (i-l) (*Cicer arietinum*) and mungbean (*Vigna radiata*) (m-p). As positive controls of CR staining, human abdominal fat biopsy tissue of a positive amyloidosis patient (q1, q2) and amyloidic fibrils of Sup35-N-terminal domain peptide (GNNQQNY) is represented (q3, q4), exhibiting green-to-red birefringence. As negative controls of the probe, sections of potato tuber as a storage organ (q5, q6) and the wheat endosperm is represented (q7, q8), where negligible birefringence is observed. Gamma values for 10X panels in CR stained images vary from 0.6-1.21, while for 40X panel, Gamma ranges from 0.5-0.9 for facilitating clear birefringence visualization, no changes in imaging parameters were done while rotating polarizer; the insets have been enhanced regarding brightness/contrast for clear presentation. (Scale bars for acid fuchsin and calcofluor stained images – 50 μm; for SEM images, scale bar – 20 μm; for ThT confocal, 10X magnification scale bar – 309.1 μm, 40X magnification scale bar – 77.3 μm; for Proteostat®, scale bar – 50 μm; for ThT and Proteostat® control images, scale bar – 50 μm; for CR staining, 10X magnification scale bar- 200 μm, 40X magnification scale bar – 50 μm; for CR control images, scale bar – 50 μm). Each experiment involves the analysis of at least three sections of three seeds of each type.

***In-silico* and biophysical characterization of seed storage protein bodies and the constituent proteins:** Since the use of combinatory amyloid-specific probes establishes the presence of

composite amyloidic assemblies in the seeds, the propensity of amyloid formation of the SSPB and their constituent proteins were analyzed by *in-silico* and biophysical approaches. As a first line of strategy, aggregation hotspot predicting software and web-servers provide insights on the likelihood of a protein to have amyloidogenic tendencies. Tango, Aggrescan and PASTA are some examples of prediction algorithms, which are successfully and extensively used to predict amyloidogenicity and aggregation-prone regions, based on previously established experimental data.(27) SSPB of aleurone and cotyledon cells contain globulins as the major component and these are well-characterized in terms of sequence and structure in comparison to albumins. Therefore, for globulins, both sequence and structural information (Uniprot and PDB) was used to predict the amyloidogenicity. However, for albumin, since structural information is not available, only sequence (Uniprot) can be used. **Figure S1 a-b** represents the secondary structure content of mungbean 8S (Uniprot Q198W5), and soybean 11S globulin (Uniprot P02858) respectively. These proteins belong to the cupin superfamily and are composed of β-barrel motifs. When the structural and sequence information of these proteins were analyzed by Aggrescan, interestingly the high aggregation-prone regions were predicted mostly in the β-barrel regions, suggesting a plausible stacking of the barrels to form amyloidic structures. A similar pattern was observed in other eukaryotic amyloidogenic proteins such as superoxide dismutase and bovine lactoglobulin (**Figure S1 c-d)**. This further suggests that the other dicots including chickpea, which have predicted β-barrel structures, would exhibit similar behaviour. On the basis of the storage functions of globulins, it can be speculated that the aggregation-prone regions might behave like sticky labels for inter-chain interactions due to close proximity to each other in the SSPB. Since for albumin proteins, structural information is not available, we used sequence from Uniprot and analysed by Aggrescan to gain insight on the number of hotspots and the total area of aggregation-prone regions. As evident from the list in **Figure S1**, the globulin proteins of both monocots and dicots show an increased propensity of hotspots compared to the albumins, further strengthening that the SSPB globulins might be the major amyloidogenic proteins.

For assaying the amyloidic signatures in the SSPB, these were isolated from the aleurone and cotyledon cells of monocots and dicots and separated from other soluble proteins (soluble fraction). Further, the two major storage proteins, globulin and albumin fractions were isolated from the SSPB. The endopeptidase, on the other hand is collected separately from seeds and is a

part of the soluble fraction. To confirm the biophysical signature, and to establish the presence of the constituent proteins in the SSPB, each of these fractions was analyzed by SDS-PAGE **(Figure S1 e)**. Dicot seed fractions were chosen for PAGE analysis since their features are well-characterized in the literature unlike the monocot proteins. The SSPB shows bands corresponding to the globulin proteins predominantly. The salt-soluble globulin fraction of mungbean and water-soluble albumin fraction, show molecular weights according to work previously done.(28, 29) The endopeptidase fraction shows two predominant bands around 80 and 55 kDa. Since germination time-based endopeptidase isolation and characterization is not well-resolved in the literature, this fraction was further validated using orthogonal assays including casein hydrolysis, as discussed in the upcoming sections.

After confirming the protein composition of the purified SSPB, these were analysed for morphological and amyloidogenic properties using SEM, dynamic light scattering (DLS), ThT, and CR. **(Figure 2 a-e)** When the SSPB of dicots **(Figure 2 a)** and monocots **(Figure 2 b)** were analysed by SEM, they show almost spherical structures in protoplasts and when isolated *in-vitro*. For mungbean, the albumin fraction shows the lowest hydrodynamic diameter of <50 nm while the globulin fraction shows an average size of 10-100 nm. The pattern however fluctuates throughout the time of analysis, probably owing to transient intermolecular interactions. The SSPB show a stable aggregated size of 500-600 nm, and fit with ultrastructural data of previous analysis **(Figure 2 c)**.(30) ThT and CR staining of the SSPB of mungbean **(Figure 2 d)** and wheat **(Figure 2 e)**, reveal green fluorescence and green-to-red birefringence, characteristic of amyloidic aggregates. The presence of ThT fluorescence in all the SSPB and CR-positive birefringence in some of these, further confirm the composite structures of the amyloids and amyloid-like assemblies.

The secondary structure analysis of proteins and their aggregates, often provide underlying differential signatures of soluble proteins vs. aggregates. Fourier-transformed infra-red spectroscopy (FTIR) serves as an important technique in this regard, as it can successfully differentiate between the α-helices, β-sheets, turns and coils. Additionally, the shifts in these signatures due to unfolding or aggregation of proteins are also reflected significantly. Therefore, the SSPB, globulins and albumins of mungbean **(Figure 2 f)** and wheat **(Figure 2 g)** were analyzed by BioATR-FTIR (Bio attenuated total reflectance-FTIR). According to the general

consensus, the α-helix signature is found at ˜1654, while β-sheets are mostly at ˜1635 and ˜1684 cm^{-1}. The signature of the β-sheet rich aggregates and amyloid fibrils are seen to be centered at ˜1610 cm^{-1} to 1632 cm^{-1} due to changes in the amide I band resulting out of interactions between β-sheets.(31) Bovine serum albumin protein was used as a control for the FTIR experiments **(Figure S1 f1)** and exhibited α-helical and β-sheet content as observed previously.(32) The albumin fraction isolated from the seeds, show predominant helical structure, followed by sheets and disordered structures.(33) The globulin fraction on the other hand shows a predominant β-sheet structure at 1632 cm^{-1} to 1633 cm^{-1} as expected from their β-barrel rich motifs. Interestingly, the SSPB not only shows the characteristic structural features of globulin, i.e. a predominant β-sheet richness, but also suggests extensive inter-sheet interactions as observed by the shift of the sheets towards 1616 cm^{-1} to 1623 cm^{-1}, indicating the presence of amyloid structures.(34) The results suggest that although the amyloids in the SSPB might be primarily composed of globulins, their signatures are distinct from globulin in their soluble state.

Since the isolated protein fractions are present in their soluble state, the next objective was to determine whether these soluble states can be converted to the *in-vivo* reconstituted amyloidic phase. To achieve this, the protein solubility is decreased by reducing the salt concentration from the mungbean globulin proteins and these were dialyzed against buffer to reduce salt concentration. The albumin fraction, which is water soluble, **(Figure 2 h1-h2)** shows no amyloidic signatures with ThT and CR after dialysis. However, the globulin fraction **(Figure 2 h3-h4)** and mixture of globulin and albumin **(Figure 2 h5-h6)** shows intense signatures of both ThT and CR, indicating that these insoluble aggregates are amyloidic assemblies. Interestingly, the same is reflected in the FTIR signatures. Dialyzed albumin shows predominant α-helical and disordered structures similar to its native state. However, dialyzed globulin shows a shift of the β-barrel structures towards 1620 cm^{-1}, indicating inter-sheet interactions in amyloidic structures. Further, a mixture of globulin and albumin, at 0 hour shows the presence of disordered structures and a minor amyloid signature. However, after incubation of 4 hours, the amyloid signature increases in intensity compared to the β-sheets and the disordered structures disappear, indicating a transition to amyloid formation **(Figure 2 i)**. Desalted BSA as a control however, shows no amyloid signature before and after dialysis. **(Figure S1 f1-f2).**

To summarize, globulin as the major constituent of SSPB exhibit aggregation-prone regions as shown by *in-silico* analysis. The SSPB exhibit ThT, CR signals and show amyloid-specific secondary structures. When the constituent fractions of SSPB are dialyzed to decrease solubility, the globulins and albumins can co-aggregate to amyloidic structures in comparison to individual proteins in their soluble state.

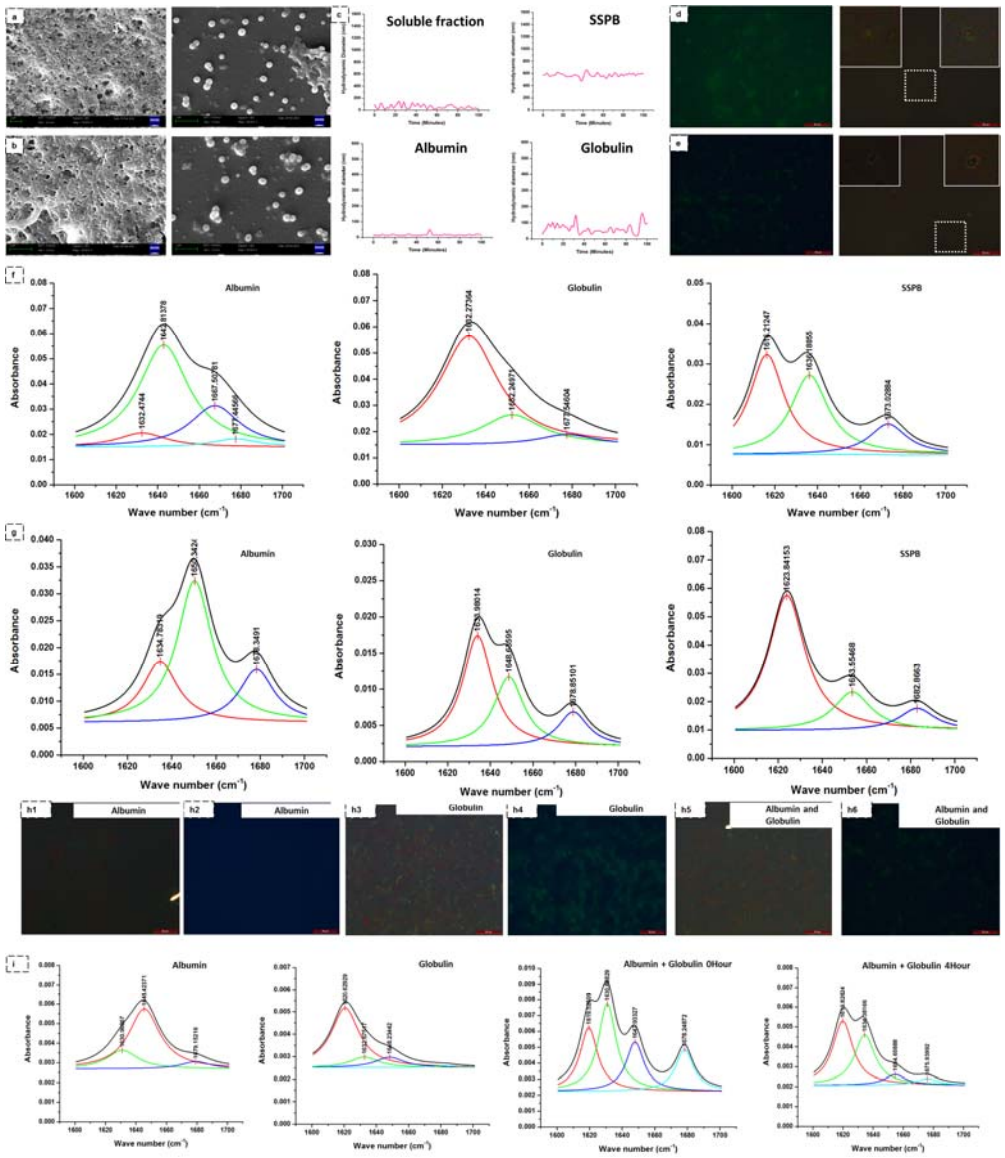

Figure 2 Analysis of the physicochemical properties of the seed storage protein bodies and constituent proteins: Representative SEM images of the dicot (a) and monocot (b) protein matrix of protoplast composed of SSPB and the isolated SSPB, reflecting on the globular shape and hydrodynamic diameter as observed in literature. DLS analysis (c) suggests that the SSPB might be composed of associated aggregates of multiple proteins as the hydrodynamic diameter is larger than any of the individual proteins. ThT and CR stained SSPB of dicot (d) and monocot (e) show signal with both the probes, confirming their amyloidic nature. FTIR analysis of the secondary structure content of water-

soluble albumin, salt-soluble globulin fraction and the SSPB of dicot (f) and monocot (g) reveal that albumin consists of helical, sheet and turn structures while globulins have predominant β-sheet signatures as evident by the major peak at 1632 cm^{-1} to 1633 cm^{-1}. The SSPB on the other hand, shows evidence of amyloids by the shift towards 1616 cm^{-1} to 1623 cm^{-1}. The albumin and globulin fractions are dialyzed next to reduce the salt concentration. Dialyzed albumin fraction of dicot does not show any CR (h1) or ThT (h2), but dialyzed globulin exhibits intense CR (h3) and ThT (h4) signals. Interestingly, dialyzed globulin and albumin when mixed together, show similar signatures (h5-h6). In FTIR analysis (i), dialyzed albumin of dicot mungbean shows the characteristic predominant helical signatures similar to native protein isolated previously. Dialyzed globulins however show a shift towards 1620 cm^{-1} of the β-sheets, suggesting intersheet interactions of globulin at lower salt concentration. On combining dialyzed globulin and albumin, the immediate signatures reveal predominant β-sheet signatures, and intermediate helical and inter-sheet interactions. But on incubation for 4 hours, the α-helix and the disordered structures decrease, while intersheet interactions become more prominent, suggesting an increase in the overall amyloid signature. (Scale bar: For SEM images, the left-panel scale bar is 2 μm, while the right-panel scale bar is 1μm; for all fluorescent and birefringence images, scale bar is 50 μm).

Functional role of amyloids during germination: To establish the role of amyloidic structures present in SSPB during seed germination, and to ascertain the possible differential stability or degradation properties of them, the monocot and dicot seeds were allowed to germinate by imbibing water. At different time-intervals, the seeds were fixed, sectioned and stained with CR and ThT to detect the changes in the amyloids and amyloid-like structures. In the wheat (monocot) seed sections, **(Figure 3 a1-c4)** the amyloid structures (CR-positive) were present till 48 hours but were not detectable at 72 and 96 hours in the aleurone cells, suggesting a possible degradation of these structures. In the mungbean (dicot) seed sections **(Figure 3 d1-e4),** the amyloids were detected upto 72 hours, suggesting that till these time-points, amyloids were not degraded to the full extent. For dicot seeds, tissue processing was not possible beyond 72 hours due to fragile nature of the seeds.

In order to detect the changes in amyloid-like structures, the seed sections were stained with ThT after allowing germination upto 96 hours in the monocots and 72 hours in the dicots. The ThT fluorescence of the seed sections was further compared to the CR fluorescence of the seed sections at the same time-points to quantify the changes in amyloid-like vs amyloid assemblies. The monocot seeds (**Figure S3 a-f)** show a decrease in ThT fluorescence intensity apparent from 4 hours in the aleurone cells. The CR fluorescence however decreases from 72 hours onwards **(Figure S3 k-p)**. Acid fuchsin staining of the germinated seed sections however depicts that the proteinaceous intensity decreases initially but then remains stable throughout as shown in (**Figure S2 a-f and k).** In the dicot seed sections **(Figure S3 g-j),** the ThT fluorescence of the

cotyledon matrix also shows a similar decrease in intensity from 24 hours, whereas the CR and acid fuchsin fluorescence remains similar till 72 hours as shown in **(Figure S3 q-t)** and (**Figure S2 g-j and l).** This shows that although amyloidic structures are degrading, the overall protein content is retained at a similar level. The results suggest that the degradation of amyloids is accompanied or preceded by an upregulation of the soluble proteins including proteases and metabolic enzymes, thus maintaining the overall protein content (35) and indicate towards a crucial role of the amyloid degradation in germination. Collectively, the CR-birefringence **(Figure 3)** and ThT-CR fluorescence dataset **(Figure S3)** reflects on the possibility of a slower degradation of amyloid structures as compared to amyloid-like aggregates. **(Supplementary Table S1)**

SEM analysis of dicot **(Figure 3 f1)** and monocot seed **(Figure 3 f3)** after 72 hours of germination shows a decrease in the overall SSPB content. The same is reflected in case of the SSPB **(Figure 3 f2 and f4)** isolated from the seeds germinated for 72 hours, where these show a heterogeneous population and decrease in size. When the SSPB and soluble fraction isolated during different germination time-points for dicot and monocot **(Figure 3 g1 and g2)** are analysed for ThT fluorescence, the soluble fraction shows baseline fluorescence. The SSPB however, show maximum fluorescence at 0 hours, which then decreases with germination, confirming loss of amyloidic characteristics. When the same SSPB from dicot **(Figure 3 h1-h2)** and monocot **(Figure 3 h3-h4)** are analysed by FTIR, the 0-hour sample shows predominant amyloidic as well as β-sheet signatures, followed by helices and turns. After 72 hours of germination, the SSPB show a decrease in the intensity of the amyloidic signatures and an increase in disordered structures, confirming amyloid degradation in germination.

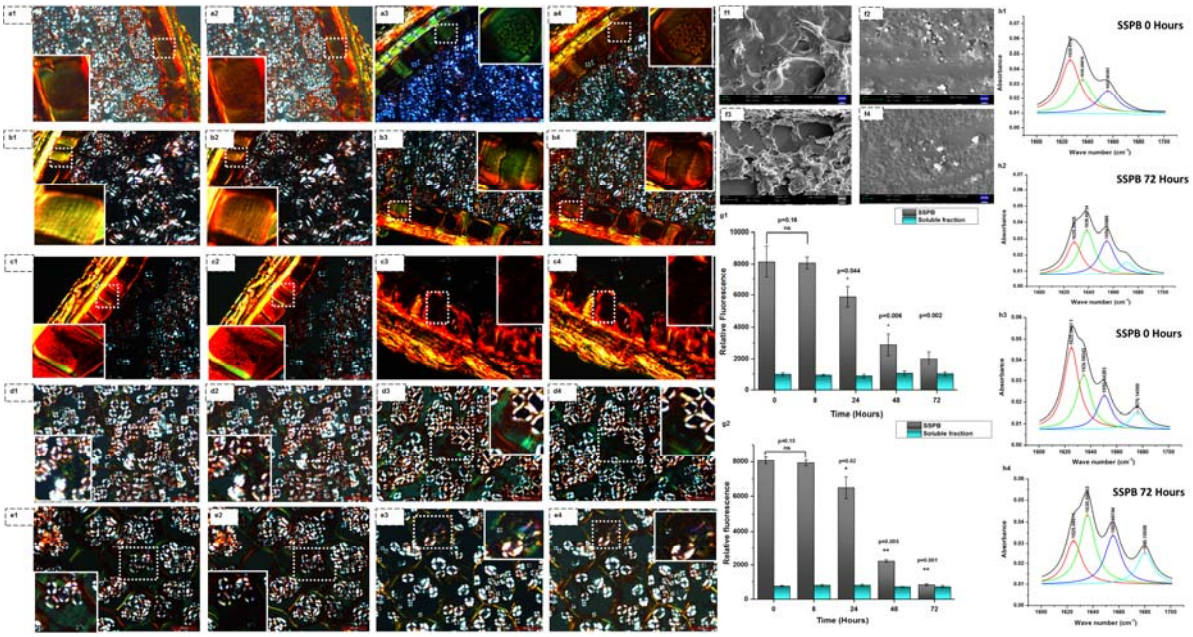

Fig 3: Congo red staining of germinated seeds and biophysical characterization of SSPB isolated from germinated seeds to detect changes in amyloid level. Congo red stained sections of wheat are represented for germination at 4 (a1-a2), 8 (a3-a4), 24 (b1-b2), 48 (b3-b4), 72 (c1-c2) and 96 (c3-c4) hours, whereas the dicot seeds were stained at 8 (d1-d2), 24 (d3-d4), 48 (e1-e2) and 72 (e3-e4) hours. In case of monocots, the amyloids are evident till 48 hours whereas in dicots, the amyloids are detected throughout all the time-points. (Gamma value for each image for CR staining is 1.3-1.6) SEM of germinated seed sections of dicot and monocot after 72 hours shows an overall decrease in the SSPB (f1 and f3). SEM analysis of the SSPB isolated from 72 hour germinated dicot and monocot seed, show a decrease in size and heterogeneous population (f2 and f4). ThT fluorescence of dicot and monocot SSPB and soluble fraction with germination, indicate the decrease in amyloidic content of the SSPB while the soluble fraction's fluorescence is maintained at a constant baseline level (g1-g2). FTIR signatures of SSPB at 0 hour and after 72 hours of germination for dicot (h1-h2) and monocot (h3-h4) show that with time, the decrease in the inter-sheet interactions in the SSPB is evident along with an increase in helices and other disordered structures, suggesting the disappearance of amyloidic character of the SSPB with germination. (Scale bar – All CR stained image scale bars correspond to 50 μm; For SEM of seed sections, scale bar of dicot corresponds to 10μm, while for monocot, scale bar corresponds to 20μm, for isolated SSPB scale bars correspond to 1μm)

Linkage of amyloid degradation during germination with upregulation and inhibition of hormones and proteases: Germination in seeds is regulated by several plant hormones such as gibberellins and abscisic acids. Gibberellin (GA) further acts downstream to regulate protease expression after seed imbibition. On the other hand, abscisic acid (ABA) acts as an inhibitor of GA and do not allow germination to initiate in presence of stress or in absence of water.(36) The initial seed proteases are plausibly present inside the SSPB and become activated by

environmental changes such as pH. These can cleave the disulphide bonds of the globulin proteins and prepare them for further cleavage. The subsequent proteases are then expressed in the cotyledon or aleurone cell cytoplasm and are assumed to cleave the storage proteins into smaller fragments. The proteases are primarily of cysteine or serine protease type and can be inhibited by protease inhibitors including phenyl methyl sulfonyl fluoride (PMSF).(37, 38) Although, the degradation of seed storage proteins in response to GA is well known, the controlling mechanism of degradation during germination is not deciphered in details previously. We hypothesize that the presence of the seed storage proteins as amyloidic assemblies, facilitates a proteostasis-dependent degradation during germination.

To gain an insight into how the amyloids are degraded in response to the hormones and proteases, the monocot and dicot seeds were imbibed in water, GA, ABA, GA and PMSF, ABA and PMSF, and PMSF alone for 72 hours. The germination percentage i.e. the percentage of seeds germinated after 72 hours was calculated. Germination was considered as positive with visible radicle emergence in mungbean and wheat. It was observed that, as compared to water, **(Figure 4 a1-a6, g-h and Figure S4 c-d)**, the seeds incubated in GA alone, **(Figure 4 b1-b6)** showed accelerated germination and decrease in amyloid signal. On the other hand, GA and PMSF treatment decreases germination percentage, and gave stronger amyloid signal compared to control **(Figure 4 c1-c6, g-h, and Figure S4 c-d)**. ABA **(Figure 4 d1-d6)** and PMSF **(Figure 4 f1-f6)** imbibition when used individually, decreases germination percentage and show increased amyloidic content when compared to control. Interestingly, a simultaneous imbibition with ABA and PMSF treatment, decreases germination further and shows maximum amyloid signatures among all treatments **(Figure 4 e1-e6, g-h and Figure S4 c-d).** Overall the CR and ThT data suggests that the degradation of the amyloid and amyloid-like composites, plays an important role in controlling germination.

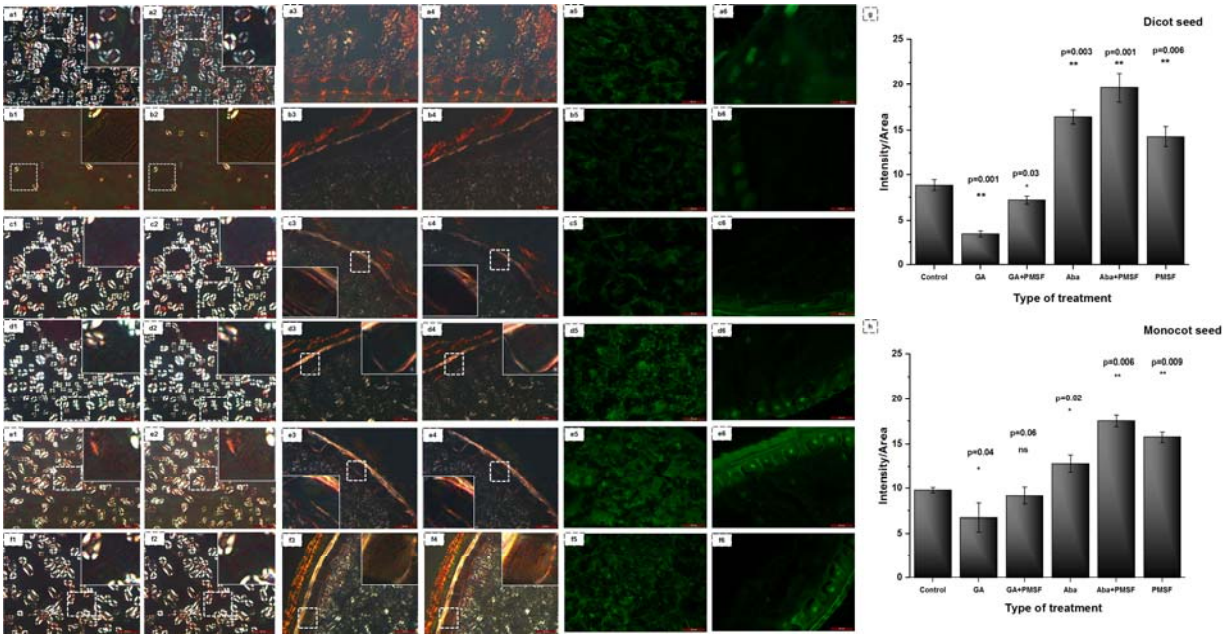

Figure 4: Exogenous treatment of monocot and dicot seeds with hormones, proteases and inhibitors and their link to amyoid degradation during germination. The mungbean (dicot) and wheat (monocot) seeds were imbibed with water (a1-a6), GA (b1-b6), GA and PMSF (c1-c6), ABA (d1-d6), ABA and PMSF (e1-e6), PMSF (f1-f6). The left four columns represent the CR stained sections of mungbean (a1-f1 and a2-f2) followed by wheat (a3-f3 and a4-f4). The right two columns represent ThT stained sections of mungbean (a5-f5) followed by wheat (a6-f6). The ThT signature intensity of the seed sections was further quantified using ImageJ and plotted (g and h), for mungbean and wheat seed respectively. Bars represent mean values with error bars as standard error of mean. (Gamma values range from 0.81-1, Scale bars for each image corresponds to 50 μm).

To further confirm the role of these signalling molecules, protoplasts were used because of their active metabolic state and absence of cell walls, leading to negligible interference of amyloid-specific dyes.(39) Firstly, the protoplasts were treated with GA, ABA and an equimolar mixture of GA and ABA. These were then stained with ThT and imaged immediately and after 2 hours. Wheat aleurone (**Figure 5 a1-a4)** and mungbean cotyledon **(Figure 5 c1-c4)** protoplasts treated with incubation buffer, GA, ABA, GA and ABA respectively at 0 hour show ThT signatures in the SSPB. The wheat (**Figure 5 b1-b4)** and mungbean (**Figure 5 d1-d4)** protoplasts after treatment for 2 hours, are again visualized for changes in ThT signature. The GA-treated protoplasts show a decrease in ThT fluorescence **(Figure 5 b2, d2, i and j)** for both monocots and dicots. The ABA treated protoplasts show a similar intensity **(Figure 5 b3, d3, i and j)** as

compared to control, whereas treatment with the mixture decreases the intensity in monocots but not in dicots **(Figure 5 b4, d4, i and j)**.

After establishing the role of the plant hormones on amyloid degradation, the effect of proteases on these structures was investigated. Purified papain was used as the control since papain-like proteases are upregulated in the seeds during germination. Further, to optimize the seed endopeptidase activity, the soluble proteins containing endopeptidase were isolated from wheat and mungbean seeds imbibed for 0, 24 and 48 hours. These fractions were then checked for enzymatic activity on casein as a standard protein. At each time-point, the amount of amino acids released due to digestion was assayed by ninhydrin. The activity of the endopeptidases isolated after 48 hours of imbibition was found to be optimum by casein hydrolysis assay, **(Figure S4)** and was characterized by SDS-PAGE **(Figure S1 e)**. The isolated protoplasts were treated with papain and endopeptidase isolated from 48h imbibed seed separately. Further the protoplasts were incubated with the same proteases but with PMSF. The dicot **(Figure 5 e1, f1)** and monocot **(Figure 5 g1, h1)** protoplasts incubated with either papain, or endopeptidase fraction, lose their amyloidic signature significantly over a period of 2 hours (**Figure 5 e2, f2, g2 and h2)**. When treated with both papain and PMSF, **(Figure 5 e3, f3, g3 and h3)** or endopeptidase and PMSF **(Figure 5 e4, f4, g4 and h4)**, the signature was retained, showing that PMSF inhibits the proteases. When the protoplasts were incubated with GA and PMSF, interestingly the signature is still retained, while GA alone leads to loss of amyloidic signatures. This confirms that GA-induced upregulation of endoproteases is countered by the presence of PMSF. **(Figure 5 e5, f5, g5 and h5)** Lastly, when the protoplasts were incubated with ABA and endopeptidase, **(Figure 5 e6, f6, g6 and h6)** the signatures lose, indicating that although ABA might be counteracting the effect of endogenous GA inside the protoplast, it cannot counter the effect of exogenous endopeptidase. The quantification is further confirmed by ImageJ **(Figure 5 k-l)**. A similar pattern is observed in the CR-stained protoplasts **(Figure S5)**. DLS analysis of the SSPB incubated with papain, and the endopeptidase fraction further exhibits the degradation of the SSPB, as evident from the decrease in the hydrodynamic diameter, while the presence of PMSF leads to maintenance of SSPB size **(Figure 5 m-n)**. The *in-situ* and *ex-vivo* results clearly indicate that a systematic degradation of the amyloid-containing SSPB is necessary for controlling germination and are linked to interplay of hormones and their downstream effectors.

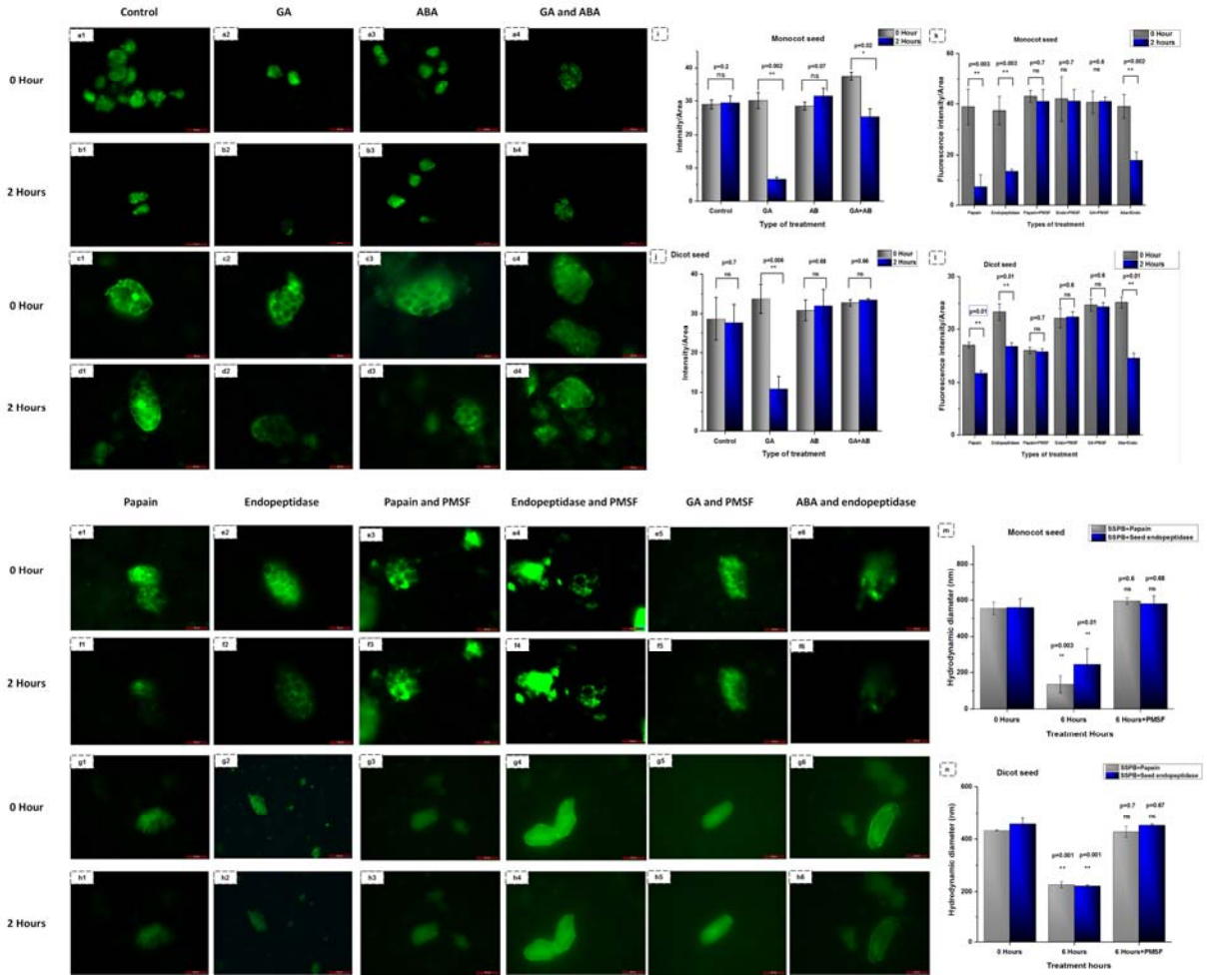

Figure 5: Effect of plant hormones and proteases on amyloidic aggregates. Wheat aleurone protoplasts treated with buffer, gibberellin (GA), abscissic acid (ABA), GA and ABA at 0 hour. (a1-a4) The protoplasts were treated for 2 hours with the same treatment and represented.(b1-b4) 0-hour mungbean cotyledon protoplasts treated with buffer, GA, ABA, GA and ABA, (c1-c4) whereas protoplasts after similar treatment of 2 hours are shown in (d1-d4). GA treatment decreases the amyloidic signal whereas ABA treatment leads to retention of fluorescence. A combined treatment of these hormones, show decrease in fluorescence in the monocots but not in dicots. The quantification of the ThT fluorescence is analysed by ImageJ and represented as (i) for wheat and (j) for mungbean. For wheat, GA alone, or simultaneous GA and ABA treatment decreases the fluorescence intensity, whereas for dicots only GA treatment is seen to decrease ThT signal. Mungbean (e1-f6) and wheat protoplasts (g1-h6) were treated with papain (e1,f1,g1,h1) endopeptidase (e2,f2,g2,h2), papain and PMSF (e3,f3,g3,h3), endopeptidase and PMSF (e4,f4,g4,h4), GA and PMSF (e5,f5,g5,h5), ABA and endopeptidase (e6,f6,g6,h6) at 0 hours and after 2 hours. The signatures were quantified and plotted in (k) and (l) for wheat and mungbean respectively. Treatment with the proteases decrease the amyloidic signatures, whereas simultaneous treatment with PMSF does not exhibit any signal decrease. GA and PMSF treatment shows a similar amyloidic signal after 2 hours, while ABA and endopeptidase treatment decreases it. DLS analysis of the SSPB with the proteases with or without PMSF are represented in (m-n). The treatment with proteases decreases the size of the SSPB, while presence of PMSF prevents the decrease in size. (Gamma value for each image is 1.3-1.6, Graphs are represented as mean with error bars as standard error of mean, Scale bars for microscopy corresponds to 50 μM)

Discussion:

Amyloids are considered as paradoxical because of their pathogenic as well as functional roles across diverse species.(40, 41) Despite plausible presence of amyloids in plants, the plant proteins investigated till now are often fibrillated at extreme conditions such as high temperature and therefore does not reflect on the behaviour of the proteins in physiological conditions. Moreover, no study has employed a combinatorial approach with latest probes such as Proteostat® and the standard CR assay for amyloid detection in plants.(16) Importantly, experimental validation using multiple amyloid-specific dyes is imperative to assign amyloid or amyloid-like properties to proteins.(14) Since the SSPB are similar to other organisms' amyloidic protein bodies in morphology and functional aspects,(11) we hypothesized that the monocot and dicot SSPB might contain amyloid structures. To establish this, we employed multiple amyloid-specific probes and fascinatingly, whereas ThT and Proteostat® bound to the entire proteinaceous regions of aleurone and cotyledon cells, the birefringent signals of amyloid due to CR staining appeared in only some areas. Thus, we conclude that SSPB in the aleurone and cotyledon cells are comprised of amyloid and amyloid-like composite structures.

To further bolster the hypothesis and to gain an insight into the amyloidogenic properties of these structures, we isolated the SSPB from the aleurone and cotyledon cells and utilized these for physicochemical studies including DLS, SEM, FTIR and reconstitution assay. The SSPB exhibit ThT and CR signatures and show prominent amyloidic signatures in IR spectra. On the other hand, the isolated protein fractions in their soluble state (globulin and albumin), are devoid of such signatures, and suggests that they assemble in the SSPB and exhibit amyloidic structure. Further, *in-silico* and reconstitution assay establishes globulins as the major amyloidogenic proteins in the SSPB and suggests that the globulin proteins can undergo extensive interaction to form amyloids and corroborate other *in-vitro* studies.(16, 42, 43)

Next, to assess the functional roles of the amyloidic structures in seed, their signatures and content was followed during the germination phases by *in-situ* techniques. The results suggest that the ThT-stained amyloid-like structures degrade faster compared to the CR-stained amyloids, possibly due to the differential stability of these two assemblies. The SSPB isolated

from germinated seeds further show a decrease in the propensity of amyloid signature by IR and establishes the degradation of the amyloids in germination.

Since, seed germination is dependent on plant hormones and proteases; we next carried out functional assay of the amyloids by employing exogenous hormones, proteases and their inhibitors. These results were further validated using protoplasts, which serve as the active metabolic state of the seed cotyledon and aleurone cells and were utilized for investigating the molecular players responsible for amyloid degradation during germination. The results indicate that on seed imbibition, GA would lead to an enhanced expression of proteases which can subsequently degrade the amyloidic structures present in the SSPB. The effect can be countered with the help of either ABA, a known antagonistic molecule of GA, or by using protease inhibitors such as PMSF. The inhibition of amyloid degradation was found to reduce the germination percentage, further confirming that amyloid degradation plays a crucial role for controlling seed germination.

Conclusion: We have shown that the monocot aleurone and dicot cotyledon seed storage protein bodies (SSPB) have composite amyloid and amyloid-like structures as proven by multiple amyloid-specific probes. The isolated SSPB were further characterized by biophysical and *in-silico* analysis and compared to their constituent fractions to show that the storage proteins adopt an amyloidic state inside the SSPB. Reconstitution of the isolated protein fractions, results in regaining of amyloidic signatures, further strengthened the hypothesis. Moreover, the amyloidic composites were shown to have a crucial role in controlling the germination percentage as shown by *in-situ*, *ex-vivo* and *in-vitro* techniques, establishing amyloids as a key player in seed physiology. Since amyloid formation follows pathways of nucleation and elongation, the same phenomenon may explain the biogenesis of the SSPB, as aggregated structures by self-seeding and cross-seeding of other protein components. The presence of these structures might facilitate protection of seeds from various environmental stresses. The current study would open up a new avenue of research to study the SSPB biogenesis and utilization at the atomic and molecular level and may illuminate the enigmatic issue of the role of functional amyloids in evolution across species.

Materials and Methods:

Materials used: CR, Thioflavin-T, acid fuchsin, purified papain were obtained from Sigma Aldrich. Proteostat® aggregation assay kit was obtained from Enzo Life Sciences. Calcofluor white, xylene, ethanol and neutral buffered formalin (4%) were procured from Thermo Scientific. Paraffin for embedding was procured from Leica. A Leica Microtome was used to obtain all the sections of 8-12 μm thickness.

Sectioning of the seeds and controls: The processing was done as per the standard protocols (44, 45) and was optimized to facilitate staining and visualization with different dyes. Briefly, the seeds were washed, surface-sterilized and incubated in 4% neutral buffered formalin at room temperature for 2 hours and transferred to 4˚C for overnight fixation. These were dehydrated with successive gradients of ethanol (30%, 50%, 70%, 90% and 100%) and permeated with paraffin. The samples were then transferred to paraffin blocks and 8 μm sections were cut. For germination study, the seeds were imbibed in cotton soaked with water in dark. After imbibition, the same procedure for fixation and processing was done. The human fat biopsy tissue and potato tubers were processed similarly. Heptapeptide GNNQQNY fibrils were first allowed to form by dissolving the monomer in 1X PBS at a concentration of 2400 μM. The formed fibrils after 8 days were spotted on glass slides and stained.

Histochemical staining of tissue sections: The processed slides were heated for 2-3 minutes at 70˚C and immediately transferred to xylene for 2 minutes in coplin jars. The slides were treated with successive gradients of ethanol (100%, 95%, and 70%) for 5 minutes each. For 95% and 70% alcohol concentrations, the treatments were repeated once. The slides were then washed with distilled water for 10 minutes.

For **SEM** analysis, after water wash, the slides were air-dried and dehydrated in a vacuum desiccator overnight. The samples were then sputter-coated with gold and visualized by Carl Zeiss Evo 18 SEM (10 kV).

For **staining**, the slides after water wash were dipped in coplin jars containing the staining solution. Acid fuchsin (0.35%) and Calcofluor white (10% v/v) stain was applied on the slides for 1 minute. Saturated solution of CR was applied for 20 minutes for amyloid detection.

Proteostat® dye was used according to the manufacturer's protocol. For ThT (20 μM) and Proteostat® staining, 10 μL of the dye was added on the tissue sections.(46)

Images were collected using Leica DM2500 fluorescent microscope equipped with cross-polarizers. ThT signal of seed sections was visualized by Leica TCS SP5 confocal system using He-Ne 488 laser (at 20% laser power) at 10X and 40X (under oil emersion). ImageJ was used for intensity analysis. The graphs were plotted using Origin Pro 9.1. For each experimental group, at three seeds were sectioned and for each probe, at least three random sections have been chosen to perform the experiments.

Isolation of protoplasts from wheat and mungbean: The protoplasts from aleurone and cotyledon cells were isolated according to previously established protocols.(47, 48) Briefly, wheat grains were dembryonated and cut into quarter grains. These were incubated in 50 mM arginine and 20 mM calcium chloride for 72 hours. The endosperm was removed from each quarter grain and the aleurone layers were incubated for 48 hours in protoplast isolation media containing 4.5% cellulase. After 48 hours, the media was replaced by protoplast incubation media and the protoplasts were freed by gentle swirling for 4 hours. For dicot seeds, 0.5 g seeds were cut into 0.5-1 mm strips and transferred immediately to 10 ml enzyme solution containing 1.2% cellulase, and incubated at room temperature in dark for 6 hours at 30 rpm. The enzyme solution was two-fold diluted with wash solution and allowed to settle. The protoplast pellet was resuspended in incubation solution at pH 5.6 and used for experiments.

Isolation and analysis of seed storage protein bodies (SSPB), soluble fraction, globulin, albumin and endopeptidase: The protoplasts were isolated first according to the above protocol and counted. A protoplast count of 10000/ml was used for SSPB isolation. These were then added to double amount of lysis buffer containing 100 mM KCl, 2 mM $MgCl_2$, 100 mM $CaCl_2$, 5 mM HEPES, 50 mM sorbitol at pH 7.2 in a chilled tube and incubated for 2 hours. The samples were analysed for protein content by ThermoFischer BCA kit as instructed by the manufacturer protocol. The samples were then layered on sucrose density gradients (20, 50 and 70%) and centrifuged at 37000 g for 1 h at 4˚C. The SSPB were isolated from 50-70% layer whereas the 20-50% layer represents the soluble proteins. Each layer was analysed for their protein content and normalized to the wet weight of the seeds.

For albumin extraction, the monocot or dicot protoplasts were lysed with double amount of lysis buffer and extracted for 2 hours in water containing 10 mM calcium chloride and 10 mM magnesium chloride, and 0.05% of Tween-80. The insoluble proteins were pelleted by centrifugation at 30000 g at 4˚C for 1 hour and the supernatant was saved as the water-soluble albumin fraction. For isolating globulin, the pellet was resuspended in Tris-HCl (10 mM) buffer, at pH 7.5 containing 10% w/v NaCl, 10 mM EDTA and again stirred for 2 hours at 4˚C. SDS-PAGE was done on a Bio-Rad mini gel electrophoresis apparatus using a 12% gel. For molecular weight composition, the calibration ladder having standard proteins from 180 to 25 kDa was used. For desalting the globulin and albumin fraction, 12 kDa and 3.5 kDa dialysis membranes were used respectively. The dialysis buffer was the extraction buffer used for isolating the proteins but without any added salts. The dialysis buffer was changed twice after an interval of 2 hours and then left on stirring overnight to ensure maximal salt removal.

For **SEM** analysis, the isolated SSPB in 1X PBS were spotted on coverslips and fixed with 0.3% glutaraldehyde for 30 minutes. After fixation, the coverslips were treated with increasing gradients of ethanol (50%, 70%, 95% and 100%) to dehydrate the samples. The samples were left overnight in a vacuum desiccator before gold-coating and performing SEM analysis. For SEM analysis of SSPB degradation, these were isolated from seeds germinated for 72 hours. For microscopy analysis, the SSPB were treated with 20 µM ThT or 1 mg/ml CR solution in water for 15 minutes and observed in Leica DM 2500 microscope. For reconstitution studies, the isolated protein fractions were dialyzed against buffer without salt using 12 kDa membrane for globulin and 3.5 kDa membrane for albumin. These were then either mixed in equal proportions or individually analysed with ThT, CR and FTIR. BSA was treated in the same way and acted as a control.

For confirming the amyloid signatures in the SSPB, these were isolated at different point of germination and were checked for ThT fluorescence at 450/489 nm. The fluorescence was compared with the soluble fraction at same time-points. The number of SSPB was normalized at each time-point to negate the effect of decrease in number of SSPB with germination. For **FTIR** analysis, a BioATR-FTIR Bruker Tensor IR-27 instrument was used. 20 µL of each sample was added to liquid nitrogen cooled ZnSe crystal and scanned from 800-4000 cm^{-1}. The secondary structure derivatives were calculated to find the peaks and Gaussian fit was performed using

Origin Pro 9.1 software. The amide bands for each spectra was then analysed for alpha and beta sheet content. **DLS analysis** was performed on Malvern Zetasizer ZS90 using a scatter angle of 90°. For each sample, 200 µl was added to DLS cuvette. Each experiment done with SSPB was repeated at least twice (n=3) with freshly prepared SSPB each time.

For **enzymatic activity** of papain and seed endoproteases, the two enzymes were incubated with casein, a standard protein at 37˚C. At fixed time-points, the proteins were precipitated with 1% tri-chloro acetic acid and centrifuged at 6000 rpm for 15 minutes. The supernatant was mixed with 5% ninhydrin solution and incubated at 60 ˚C for 30 minutes. The samples were then analysed for absorbance at 560 nm using Perkin Elmer Elisa plate reader.

Treatment of the seeds and protoplasts with exogenous molecules and their inhibitors: For functional relevance of the amyloids in seed germination, the wheat and mungbean seeds were imbibed in GA, GA and PMSF, ABA, ABA and PMSF and PMSF alone for 72 hours. All the treatments were added at a final concentration of 50 µM. The seeds were then fixed and processed and CR-ThT staining was performed to check amyloid retention. In separate set of experiments, 30 seeds were imbibed in similar treatment for 72 hours and the germination percentage was calculated. The monocot and dicot protoplasts were treated with GA, ABA, GA and ABA, papain, seed endopeptidase, papain and PMSF, endopeptidase and PMSF, GA and PMSF, ABA and endopeptidase at the same final concentration of 50 µM for 2 hours. The protoplasts were stained with ThT or CR and visualized to check amyloid signals. For ThT staining, live protoplasts were added on coverslips with enough protoplast incubation buffer to avoid drying. 20 µM ThT solution was added on the coverslips and the protoplasts were monitored for 2 hours using Leica DM 2500 fluorescent microscope. For CR staining, the protoplasts were fixed in a fixative solution containing 2.5:2.5:5 of water:acetic acid:ethanol and 0.36 g sorbitol per 10 ml of fixative. After fixation of 30 minutes, the protoplasts were stained with saturated CR solution for 10 minutes and observed through Leica DM 2500 birefringence analyser. Each experiment done with protoplasts was repeated at least twice (n=3) with freshly prepared protoplasts each time. 30 seeds in each group were treated separately and allowed to germinate for 72 hours. The germination index was then calculated as the % of number of germinated seeds.

Computational analysis: The secondary structure content of each protein was performed by Uniprot, PDB, Pfam and JPred web servers. Aggrescan webserver was used to predict the potential amyloidogenic aggregation-prone regions in each of these sequences.

Statistical and image analysis: Origin Pro 9.1 was used to plot all the graphs and t-test was used to analyse the statistical significance between the data pairs. ImageJ and Leica Las X software were used to analyse the microscopy images. Each experiment is performed at least thrice (n=3) to obtain statistically significant results.

References:

1. Shewry PR, Halford NG. Cereal seed storage proteins: structures, properties and role in grain utilization. Journal of experimental botany. 2002;53(370):947-58.
2. Shewry PR, Napier JA, Tatham AS. Seed storage proteins: structures and biosynthesis. The Plant cell. 1995;7(7):945-56.
3. Nadaud I, Tasleem-Tahir A, Chateigner-Boutin A-L, Chambon C, Viala D, Branlard G. Proteome evolution of wheat (Triticum aestivum L.) aleurone layer at fifteen stages of grain development. Journal of Proteomics. 2015;123:29-41.
4. Reyes FC, Chung T, Holding D, Jung R, Vierstra R, Otegui MS. Delivery of Prolamins to the Protein Storage Vacuole in Maize Aleurone Cells. The Plant Cell. 2011;23(2):769-84.
5. Isaienkov SV. [Plant vacuoles: physiological roles and mechanisms of vacuolar sorting and vesicular trafficking]. TSitologiia i genetika. 2014;48(2):71-82.
6. Hughes JS, Swanson B. MICROSTRUCTURE OF LENTIL SEEDS (Lens Culinaris). Food Structure. 1986;5:8.
7. Derbyshire E, Wright DJ, Boulter D. Legumin and vicilin, storage proteins of legume seeds. Phytochemistry. 1976;15(1):3-24.
8. Craig S, Millerd A. Pea seed storage proteins — Immunocytochemical localization with protein a-gold by electron microscopy. Protoplasma. 1981;105(3):333-9.
9. Herman E, Schmidt M. Endoplasmic Reticulum to Vacuole Trafficking of Endoplasmic Reticulum Bodies Provides an Alternate Pathway for Protein Transfer to the Vacuole. Plant Physiology. 2004;136(3):3440-6.
10. Schmidt SR. Protein Bodies in Nature and Biotechnology. Molecular Biotechnology. 2013;54(2):257-68.
11. Narayanaswamy R, Levy M, Tsechansky M, Stovall GM, O'Connell JD, Mirrielees J, et al. Widespread reorganization of metabolic enzymes into reversible assemblies upon nutrient starvation. Proceedings of the National Academy of Sciences. 2009;106(25):10147-52.
12. Peters LZ, Karmon O, David-Kadoch G, Hazan R, Yu T, Glickman MH, et al. The Protein Quality Control Machinery Regulates Its Misassembled Proteasome Subunits. PLOS Genetics. 2015;11(4):e1005178.
13. Benson MD, Buxbaum JN, Eisenberg DS, Merlini G, Saraiva MJM, Sekijima Y, et al. Amyloid nomenclature 2020: update and recommendations by the International Society of Amyloidosis (ISA) nomenclature committee. Amyloid : the international journal of experimental and clinical investigation : the official journal of the International Society of Amyloidosis. 2020;27(4):217-22.

14. Matiiv AB, Trubitsina NP, Matveenko AG, Barbitoff YA, Zhouravleva GA, Bondarev SA. Amyloid and Amyloid-Like Aggregates: Diversity and the Term Crisis. Biochemistry (Moscow). 2020;85(9):1011-34.
15. Antonets KS, Nizhnikov AA. Amyloids and prions in plants: Facts and perspectives. Prion. 2017;11(5):300-12.
16. Antonets KS, Belousov MV, Sulatskaya AI, Belousova ME, Kosolapova AO, Sulatsky MI, et al. Accumulation of storage proteins in plant seeds is mediated by amyloid formation. PLoS Biol. 2020;18(7):e3000564.
17. Guo WJ, Ho TH. An abscisic acid-induced protein, HVA22, inhibits gibberellin-mediated programmed cell death in cereal aleurone cells. Plant Physiol. 2008;147(4):1710-22.
18. Herrera-Ubaldo H, de Folter S. Exploring Cell Wall Composition and Modifications During the Development of the Gynoecium Medial Domain in Arabidopsis. Frontiers in Plant Science. 2018;9(454).
19. Kesari V, Rangan L. Coordinated changes in storage proteins during development and germination of elite seeds of Pongamia pinnata, a versatile biodiesel legume. AoB Plants. 2011;2011:plr026-plr.
20. Boke E, Ruer M, Wühr M, Coughlin M, Lemaitre R, Gygi SP, et al. Amyloid-like Self-Assembly of a Cellular Compartment. Cell. 2016;166(3):637-50.
21. Oshinbolu S, Shah R, Finka G, Molloy M, Uden M, Bracewell DG. Evaluation of fluorescent dyes to measure protein aggregation within mammalian cell culture supernatants. J Chem Technol Biotechnol. 2018;93(3):909-17.
22. Laor D, Sade D, Shaham-Niv S, Zaguri D, Gartner M, Basavalingappa V, et al. Fibril formation and therapeutic targeting of amyloid-like structures in a yeast model of adenine accumulation. Nature Communications. 2019;10(1):62.
23. Ghosh S, Khanra D, Krishna V, Thakur AK. Wild type transthyretin cardiac amyloidosis in a young individual: A case report. Medicine (Baltimore). 2021;100(17):e25462-e.
24. Shewry PR. Tuber storage proteins. Annals of botany. 2003;91(7):755-69.
25. Yakupova Elmira I, Bobyleva Liya G, Vikhlyantsev Ivan M, Bobylev Alexander G. Congo Red and amyloids: history and relationship. Bioscience Reports. 2019;39(1).
26. Murphy CL, Eulitz M, Hrncic R, Sletten K, Westermark P, Williams T, et al. Chemical typing of amyloid protein contained in formalin-fixed paraffin-embedded biopsy specimens. American journal of clinical pathology. 2001;116(1):135-42.
27. Belli M, Ramazzotti M, Chiti F. Prediction of amyloid aggregation in vivo. EMBO Rep. 2011;12(7):657-63.
28. Kusumah J, Real Hernandez LM, Gonzalez de Mejia E. Antioxidant Potential of Mung Bean (Vigna radiata) Albumin Peptides Produced by Enzymatic Hydrolysis Analyzed by Biochemical and In Silico Methods. Foods. 2020;9(9):1241.
29. Mendoza EMT, Adachi M, Bernardo AEN, Utsumi S. Mungbean [Vigna radiata (L.) Wilczek] Globulins: Purification and Characterization. Journal of Agricultural and Food Chemistry. 2001;49(3):1552-8.
30. Van der Wilden W, Herman EM, Chrispeels MJ. Protein bodies of mung bean cotyledons as autophagic organelles. Proceedings of the National Academy of Sciences of the United States of America. 1980;77(1):428-32.
31. Waeytens J, Mathurin J, Deniset-Besseau A, Arluison V, Bousset L, Rezaei H, et al. Probing amyloid fibril secondary structures by infrared nanospectroscopy: experimental and theoretical considerations. Analyst. 2021;146(1):132-45.
32. Ahmad F, Zhou Y, Ling Z, Xiang Q, Zhou X. Systematic Elucidation of Interactive Unfolding and Corona Formation of Bovine serum albumin with Cobalt Ferrite Nanoparticles. RSC Advances. 2016;6.

33. Moreno FJ, Clemente A. 2S Albumin Storage Proteins: What Makes them Food Allergens? Open Biochem J. 2008;2:16-28.
34. Sarroukh R, Goormaghtigh E, Ruysschaert J-M, Raussens V. ATR-FTIR: A “rejuvenated” tool to investigate amyloid proteins. Biochimica et Biophysica Acta (BBA) - Biomembranes. 2013;1828(10):2328-38.
35. Han C, Yin X, He D, Yang P. Analysis of Proteome Profile in Germinating Soybean Seed, and Its Comparison with Rice Showing the Styles of Reserves Mobilization in Different Crops. PLOS ONE. 2013;8(2):e56947.
36. Shu K, Zhou W, Chen F, Luo X, Yang W. Abscisic Acid and Gibberellins Antagonistically Mediate Plant Development and Abiotic Stress Responses. Frontiers in Plant Science. 2018;9.
37. Jinka R, Rao PR. Storage protein degradation in germinating horse gram seeds. Indian journal of plant physiology. 2002;7:314-20.
38. Otegui MS, Herder R, Schulze J, Jung R, Staehelin LA. The proteolytic processing of seed storage proteins in Arabidopsis embryo cells starts in the multivesicular bodies. The Plant cell. 2006;18(10):2567-81.
39. Jacobsen JV, Zwar JA, Chandler PM. Gibberellic-acid-responsive protoplasts from mature aleurone of Himalaya barley. Planta. 1985;163(3):430-8.
40. Bleem A, Daggett V. Structural and functional diversity among amyloid proteins: Agents of disease, building blocks of biology, and implications for molecular engineering. Biotechnology and Bioengineering. 2017;114(1):7-20.
41. Kumar V, Sinha N, Thakur AK. Necessity of regulatory guidelines for the development of amyloid based biomaterials. Biomaterials science. 2021;9(12):4410-22.
42. Zhou J, Li T, Peydayesh M, Usuelli M, Lutz-Bueno V, Teng J, et al. Oat Plant Amyloids for Sustainable Functional Materials. Advanced Science. 2022;9(4):2104445.
43. Tang C-H, Zhang Y-H, Wen Q-B, Huang Q. Formation of Amyloid Fibrils from Kidney Bean 7S Globulin (Phaseolin) at pH 2.0. Journal of Agricultural and Food Chemistry. 2010;58(13):8061-8.
44. Jääskeläinen A-S, Holopainen-Mantila U, Tamminen T, Vuorinen T. Endosperm and aleurone cell structure in barley and wheat as studied by optical and Raman microscopy. Journal of Cereal Science. 2013;57(3):543-50.
45. Wood JA, Knights EJ, Choct M. Morphology of Chickpea Seeds (Cicer arietinum L.): Comparison of desi and kabuli Types. International Journal of Plant Sciences. 2011;172(5):632-43.
46. Navarro S, Ventura S. Fluorescent dye ProteoStat to detect and discriminate intracellular amyloid-like aggregates in Escherichia coli. Biotechnol J. 2014;9(10):1259-66.
47. Taiz L, Jones RL. The isolation of barley-aleurone protoplasts. Planta. 1971;101(2):95-100.
48. Ahmed MAA, Miao M, Pratsinakis ED, Zhang H, Wang W, Yuan Y, et al. Protoplast Isolation, Fusion, Culture and Transformation in the Woody Plant Jasminum spp. Agriculture. 2021;11(8):699.